International Journal of Chemical Kinetics

WILEY

RESEARCH ARTICLE

A Green Approach to Silver Nanoparticle Synthesis Using *Glycyrrhiza glabra* to Investigations Antimicrobial Applications

Muhammad Junaid[1] | H. M. Ameen Soomro[2] | Abdul Qadir Ahmad[3] | Sehrish Faiz[4] | Nouman Ali Shahid[2] | Mahmood Basil A. Al-Rawi[5] | Muhammad Amjad Riaz[6] | Mohd Arif Dar[7] | Mohammed El-Meligy[8,9] | Irfanullah Khan[10]

[1]Institute of Physics, The Islamia University of Bahawalpur, Bahawalpur, Pakistan | [2]Khwaja Fareed University of Engineering and Information Technology (KFUEIT), Rahim Yar Khan, Pakistan | [3]Institute of Chemistry, Government College University Lahore, Lahore, Pakistan | [4]Department of Chemistry, Forman Christian College, University Lahore, Lahore, Pakistan | [5]Department of Optometry, College of Applied Medical Sciences, King Saud University, Riyadh, Saudi Arabia | [6]Department of Chemistry, University of Education Lahore, Vehari, Pakistan | [7]Faculty of Allied Health Sciences, Chettinad Hospital and Research Institute, Chettinad and Education, Kelambakkam, Tamil Nadu, India | [8]Jadara University Research Centre, Jadara University, Irbid, Jordan | [9]Applied Science Research Center, Applied Science Private University, Amman, Jordan | [10]Department of Integrative Biology, The College of Arts and Sciences, Oklahoma State University, USA

Correspondence: Muhammad Junaid (mjunaid310@yahoo.com)

Received: 16 December 2024 | **Revised:** 8 February 2025 | **Accepted:** 7 April 2025

Funding: This study was supported by King Saud University, Riyadh, Saudi Arabia, through the Researchers Supporting Project number (RSP2025R378).

ABSTRACT

This study focuses on the green synthesis and characterization of silver nanoparticles (Ag-NPs) using *Glycyrrhiza glabra* root extract as a natural reducing agent. The antimicrobial potential of these nanoparticles was evaluated against a range of pathogens, including both bacteria and fungi. The synthesis process was initiated by adding *Glycyrrhiza glabra* root extract to a silver nitrate solution, resulting in a distinct color change from colorless to dark yellow, and eventually to black, signaling the formation of Ag-NPs. The formation and properties of the nanoparticles were further confirmed through UV–visible spectroscopy, which revealed a strong surface plasmon resonance peak at 421 nm, characteristic of Ag-NPs. X-ray diffraction (XRD) analysis showed that the nanoparticles possessed a face-centered cubic (FCC) structure, confirmed by the observation of well-defined Bragg reflections. Additionally, Energy Dispersive x-Ray Spectroscopy (EDX) and scanning electron microscopy (SEM) analyses were performed to assess the elemental composition and morphology of the synthesized nanoparticles. EDX results confirmed the presence of silver, while SEM images revealed the presence of nanoparticle aggregates, though no distinct morphology was observed. The antimicrobial activity of the synthesized Ag-NPs was tested against both Gram-positive and Gram-negative bacteria, with results indicating a significantly stronger antimicrobial effect against Gram-negative bacteria. These findings highlight the promising potential of green-synthesized Ag-NPs as effective antimicrobial agents, providing a sustainable and eco-friendly approach to nanoparticle synthesis with significant implications for various biomedical applications.

1 | Introduction

Nanotechnology is a rapidly growing field of study in modern materials science, particularly in biotechnology [1]. Noble metal nanoparticles are now being employed in a wide range of applications in biology, medicine, physics, chemistry, and material science. Ag-NPs are the most marketable nanoparticles among nanostructured noble metals (AgNPs) [2]. The use of AgNPs in molecular imaging, drug delivery, photonics, microelectronics, biomedicine, and biosensors has gotten a lot of interest. AgNPs have been developed using a variety of physical and chemical approaches all around the world [3]. The use of environmentally friendly materials such as plant extracts, bacteria, and fungi for nanoparticle synthesis has received a lot of attention in recent years, and green synthesis of metal nanoparticles has succeeded in getting a lot of attention because of its numerous advantages over other chemical and physical methods [4]. Green synthesis is a simplistic and effective approach for producing nanoparticles with high stability and size [5]. Plant-mediated nanoparticle synthesis is chosen because it allows for the production of vast quantities of nanoparticles at a low cost; it is also environmentally benign and safe for human therapeutic use [5]. Because of the diversity and great potential of plants in creating nanoparticles of various forms, this topic continues to receive a lot of attention [5].

Many novel antibiotics have been developed by pharmaceutical companies during the previous three decades [6]. Microorganisms, on the other hand, have developed resistance to these medications. Microbial resistance is becoming more of an issue, and the future usage of antimicrobial medications is still questionable. The creation and modification of novel antimicrobial agents (e.g., natural and inorganic-based antimicrobial compounds) are required due to the rising bacterial resistance to traditional antibiotics, because of its antibacterial action, investigations on AgNPs have grown in popularity in recent years [7, 8]. Because of their antibacterial qualities, AgNPs are used in a range of industries such as medicine, industry, animal husbandry, packaging, cosmetics, health, and military applications. Green production of novel AgNPs with active antibacterial properties is advantageous [8]. The primary goal of this study was to develop a unique methodology for green chemistry biosynthesis of AgNPs utilizing an aqueous extract of *Glycyrrhiza glabra* roots at room temperature [8]. The synthesized nanoparticles were characterized by UV–visible spectroscopy, x-ray diffraction (XRD), scanning electron microscope (SEM), and energy dispersive spectroscopy [9]. The antibacterial efficacy of synthesized AgNPs against Gram-negative *Escherichia coli* and Gram-negative *Staphylococcus aureus* was evaluated. The antibacterial activity of synthesized Ag-NPs is found to be more efficient against Gram-negative (*E. coli*) bacteria than Gram-positive bacteria (*S. aureus*) [10–12].

2 | Results and Discussion

The precursor solution, silver nitrate, and sodium hydroxide were bought from Sigma Aldrich and 99% purity was used for the preparation of the sample. Beakers and other glassware, which were washed with ethanol from Sigma Aldrich, were used. To prepare plant extract, *Glycyrrhiza glabra* roots were used.

2.1 | Preparation of Plant Extract

To prepare plant extracts, *Glycyrrhiza glabra* roots were used. Initially, all the glassware items being used were washed with ethanol. To remove any impurities and dust, it was properly washed with distilled water. For proper drying of *Glycyrrhiza glabra* roots, the beaker was covered properly with a plastic sheet to avoid dust and impurities present in the open air. The beaker was placed under the sun for about 3 days to dry *Glycyrrhiza glabra* roots properly. The *Glycyrrhiza glabra* roots were then ground and converted into a fine powder. An aqueous plant extract was prepared by weighing 10 g of *Glycyrrhiza glabra* powder on a weight balance. One hundred milliliters of distilled water was poured into a 200-mL beaker. Ten grams of *Glycyrrhiza glabra* powder was then mixed with 100 mL of distilled water using a hot plate for proper mixing at 550°C with 1000 rpm for 30 min. To separate any solid particles from the liquid, the solution was then filtered using Whatman filter paper, and the filtered solution was then placed at room temperature for 1 h. The plant extract was prepared and ready to be used as a reducing and stabilizing agent [13, 14].

2.2 | Synthetization of Ag-NPs

To prepare Ag-NPs, 0.8579 g of $AgNO_3$ and 0.2062 g of NaOH were dissolved in 100-mL deionized or distilled water. NaOH is used to maintain the pH of the prepared solution. The prepared samples were placed on a hot plate and the temperature of the hot plate was set at 250°C and stirred at the rate of 800 rpm. Ten milliliters of plant extract was taken and mixed into the solution of ($AgNO_3$). After 1 h, the prepared solution was completely mixed and the color of the sample was changed to dark brown. The initial pH of the solution was 7, to increase the pH, a 0.1-mol/L solution of NaOH was added dropwise till the pH was maintained at 11, and the color of the solution started changing from dark brown to dark black. The solution was placed overnight and the black NPs of Ag precipitated in the bottom of the beaker. To collect the Ag-NPs precipitated in the beaker, the centrifugation process was used. The NPs of Ag in black color precipitated on the bottom were first separated from the remaining solution. The Ag-NPs solution was then evenly shifted in centrifuge tubes. The centrifuge machine was set for centrifugation at a rate of 6500 rpm for 15 min. The Ag-NPs were dried in an oven at 500°C for 5 h. The solid Ag-NPs were then crushed using a crusher and converted into dry powder.

2.3 | XRD Analysis

The confirmation of Ag-nanoparticles is analysed through a Bruker D8 Advance powder x-ray diffractometer with Cu Kα (λ = 1.5406 Å) radiation 04-0783. The XRD peaks are compared with the standard card (JCPDS card no. 04-0783) to confirm the formation of prepared sample. When performing XRD on Ag nanoparticles, the resulting diffraction pattern typically exhibits sharp peaks corresponding to the face-centered cubic (FCC) structure of metallic silver. A high-intensity peak for FCC materials is the [111] reflection, which was detected in the sample along with other peaks whose intensities reflected the high degree of crystallinity of AgNPs synthesized from *Glycyrrhiza glabra* aqueous root extract. This feature further enhances AgNPs' antimicrobial capabilities [15, 16].

The crystallite size of Ag nanoparticles can be calculated using the Scherrer equation as follows:

$$D = k\lambda/\beta\cos\theta \tag{1}$$

The peak broadening of diffraction peaks revealed that AgNPs' small crystallite size was found to be 41.065 nm via the Sherrer formula, and the lattice parameter value is 4.048 Å.

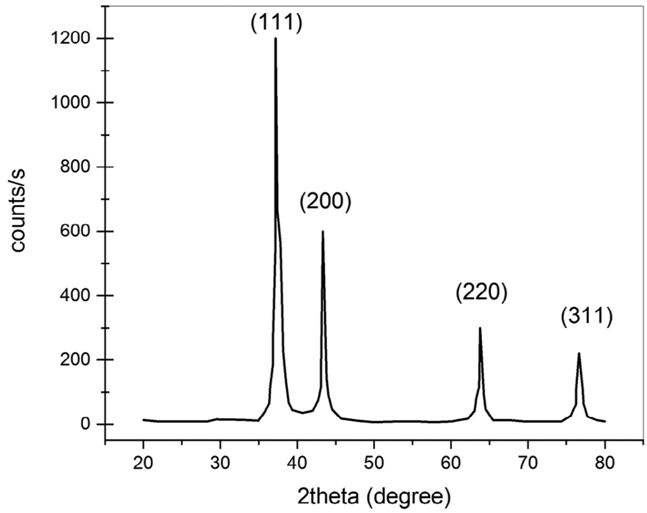

FIGURE 1 | AgNPs produced from *Glycyrrhiza glabra* root extract XRD pattern.

When performing XRD on Ag nanoparticles, the resulting diffraction pattern typically exhibits sharp peaks corresponding to the FCC structure of metallic silver as shown in Figure 1.

2.4 | SEM Analysis

The SEM (Cube II Emcraft South Korea) setup is used to study the surface structure of samples, showing particle arrangements at different scan rates. Figure 2a shows the micrographs of synthesized *Glycyrrhiza glabra* root extract of Ag-NPs on a scale of 500 nm. The micrograph shows small spherical-shaped nanoparticles combined to form large agglomerates of different shapes and sizes. In Figure 2a, the size of nanoparticles is calculated at different positions on the micrograph. The positions are selected where the spherical shape is visible. The spherical nanoparticle with tag C_1 has a diameter of 86.80 nm. Similarly, the spherical nanoparticle with tag C_2 has a diameter of 69.63 nm. Spherical-shaped nanoparticles with tags C_3 and C_4 have a diameter of 88.92 and 79.63 nm. The nanoparticles are of different sizes, with a size range from 60 to 90 nm. Figure 2b shows the micrographs of synthesized Ag-NPs on 500-nm scales; the micrograph again shows similar results. The micrograph shows some space between the large agglomerates formed by the combination of small spherical-shaped nanoparticles. Also, the shapes of the agglomerates have no proper pattern. Figure 2c shows the micrographs on a 1-μm scale. This micrograph again shows a large agglomeration of Ag-NPs with no proper shape. Ag-NPs of spherical shape and composite nanoparticles with improper shapes are more visible [17–19]. The agglomeration is due to a long-time gap during synthesis and characterization. Figures 2d and 2e showed the micrographs on a 5-m scale and a 10-μm scale, respectively.

SEM micrographs confirm the spherical-shaped small nanoparticles visible on the surface and different sizes and improperly shaped agglomerates because of the combination of small nanoparticles. SEM micrographs reveal individual spherically shaped AgNPs as well as a variety of aggregates. Individual nanoparticles have a particle size of roughly 60–90 nm. These nanoparticles are stable and not in direct touch, according to SEM images. This could be due to the capping agent's ability to stabilize the nanoparticles. There were also large aggregates of nanoparticles with an uneven structure and no well-defined shape. Figure 2f shows an irregularly shaped nanoparticle with an average size of 81.24 nm.

TABLE 1 | EDX weight ratio.

Element	Weight	Atomic
O K	22.29	65.92
Ag L	77.71	34.08
Total	100.00	

SEM also provides information about the surface texture of the nanoparticles. In the case of Ag-NPs synthesized using plant extracts, the surface may exhibit a slight roughness or a thin organic coating. This coating is often due to the presence of biomolecules from the extract that act as capping agents, stabilizing the nanoparticles. These surface characteristics can play a role in the interaction of the nanoparticles with other materials, such as cells in biomedical applications [20, 21].

Nanoparticle morphology plays a crucial role in determining their antimicrobial properties. By tailoring the size, shape, surface charge, and functionalization of nanoparticles, their effectiveness against various pathogens can be optimized and the morphology of Ag-NPs changes with increasing scan rate because of differences in the kinetics of nanoparticle formation, nucleation and growth processes, aggregation tendencies, and the overall reaction dynamics. These morphological changes can influence the efficiency of the nanoparticles, including their antimicrobial properties.

2.5 | EDX Spectroscopy

The elemental analysis of the bio-synthesized nanoparticles is revealed by the EDX and it confirmed the production of Ag-NPs.

The production of Ag-NPs is confirmed by energy-dispersive x-ray analysis, which reveals a strong signal in the silver region (Figure 3).

Due to surface plasmon resonance (SPR), metallic silver nanocrystals have a characteristic optical absorption peak at 3 keV, which is typical of silver nanocrystallites absorption, suggesting the existence of AgNPs [22]. Surprisingly, an adjoint element, oxygen, was discovered. As EDX is a surface technique, the observed oxygen peaks are due to the contact of the sample with the environment or may be due to the organic compounds present in the extract, which were used for the synthesis of AgNPs as reported in Table 1

According to the research, the nano-structures were found to be entirely made of silver. Different locations were focused during the EDX analysis, and the relevant peaks are displayed in Figure 3. Ag and O made up 77.7 and 22.29 weight percent of the sample, respectively. The details of the EDX spectra of the Ag-NPs values measured in atomic and weight percent are

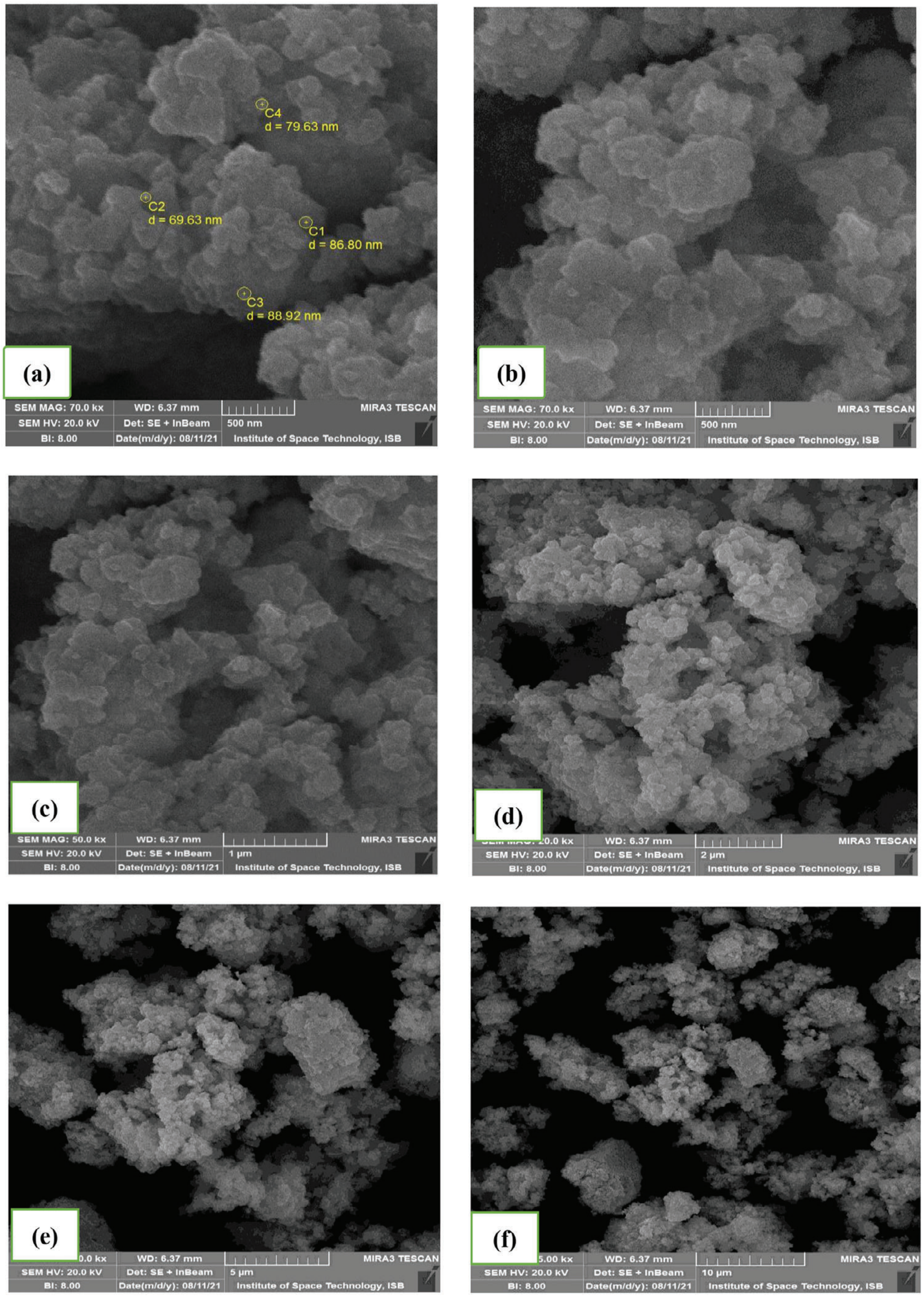

FIGURE 2 | (a–f): SEM images of Ag at different resolutions.

listed in Table 1. The image reveals the shape, morphology, and size of nanoparticles. Small, spherically shaped Ag-NPs combine to form agglomerates of irregularly shaped nanoparticles. The average size of spherically shaped silver synthesized from aqueous extracts of *Glycyrrhiza glabra* is 81.24 nm. The existence of large-sized agglomerates with uneven structures suggests that the protracted incubation period caused aggregation [22, 23].

2.6 | UV–Vis Analysis

A UV–Vis–NIR spectrophotometer (Shimadzu UV2600 plus) equipped with an integrating sphere was used to assess the optical absorption and transmission of the prepared sample as shown in Figure 4. The UV–visible spectrum was used to track the reduction of pure silver ions from a wavelength of 200–800 nm. There are various wavelengths of UV–Vis light absorbed and stimulated by nanoparticles owing to charge density at the interface between the conductor and insulator.

Figure 4 shows a single strong distinctive absorption peak at 421 nm in the UV–visible spectra. The SPR peak of AgNPs corresponds to this absorption peak.

Glycyrrhiza glabra root extract has proven to be an effective green-reducing agent for the synthesis of Ag-NPs. The UV–Vis

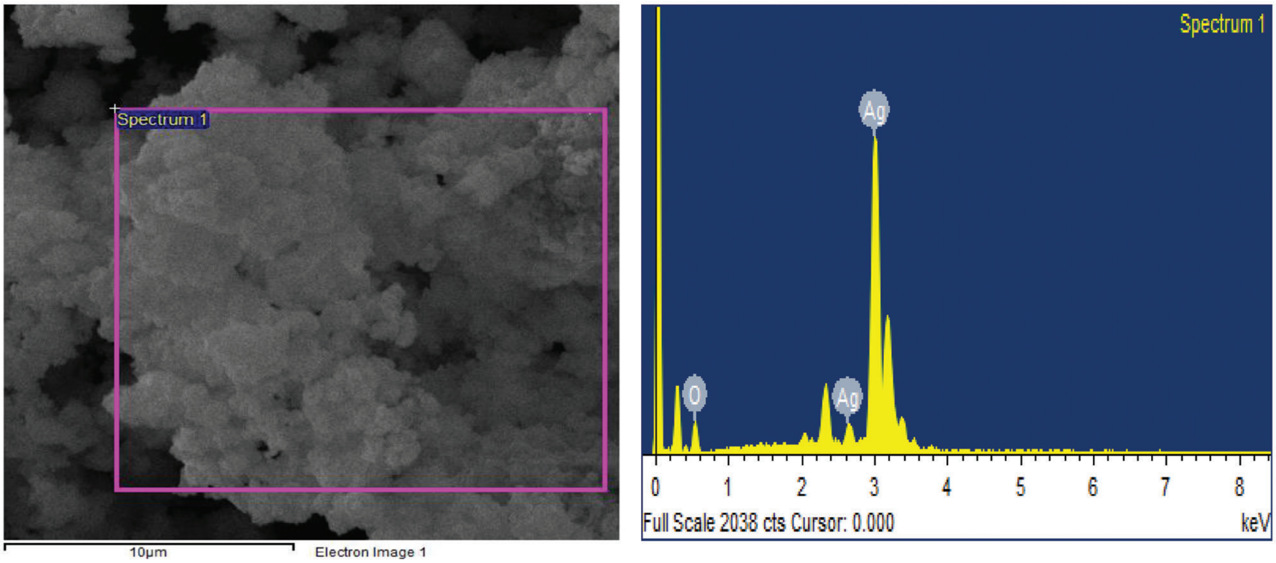

FIGURE 3 | EDX analysis of AgNPs.

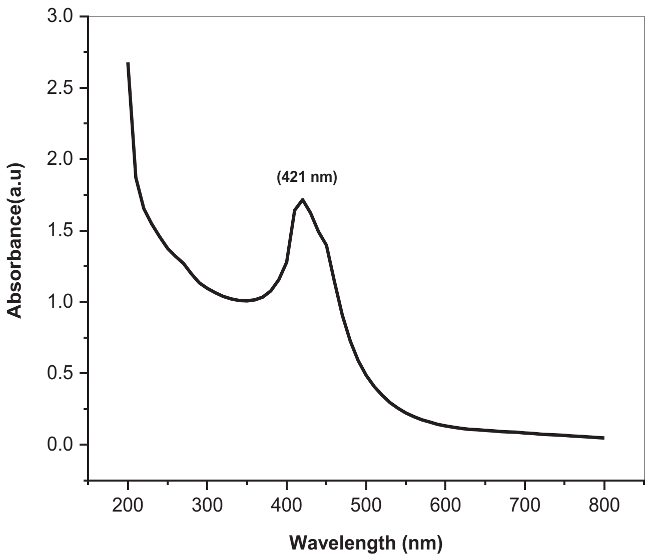

FIGURE 4 | UV spectra of Ag-NPs.

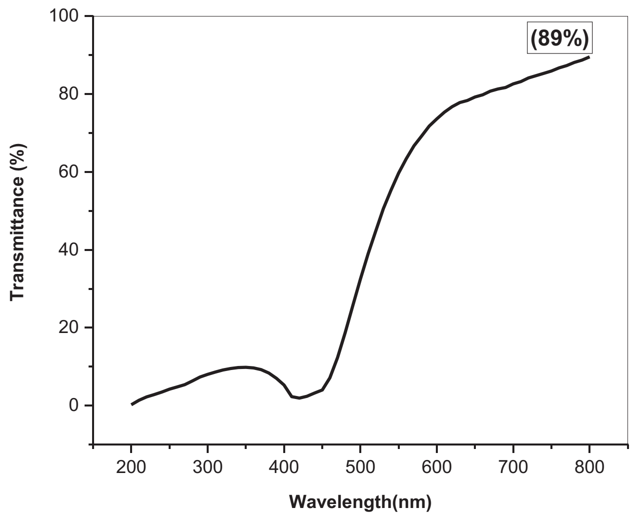

FIGURE 5 | Transmittance spectra of Ag-nanoparticles.

spectroscopy results demonstrated a well-defined SPR peak at 421 nm, confirming the formation of monodispersed AgNPs. This eco-friendly synthesis method could be further explored for its potential applications in biomedicine and environmental remediation [24–26].

2.7 | Transmittance

A UV–Vis spectrophotometer records the percentage of light transmitted through the colloidal solution of AgNPs in the range of 200–800 nm as reported in Figure 5. Typically, for Ag-NPs, the transmittance decreases in the visible region where the SPR peak is observed, which often lies between 400 and 450 nm. This decrease in transmittance corresponds to the characteristic absorbance of Ag-NPs. The UV–Vis transmittance spectrum generally shows a significant reduction in transmittance around the SPR peak (around 421 nm), where the nanoparticles absorb light. Beyond the SPR region, the transmittance increases, particularly in the UV region, indicating that the nanoparticles allow light to pass through at these wavelengths [27]. The degree of transmittance is affected by several factors, including the size and concentration of the nanoparticles in the solution. Smaller nanoparticles or more dilute solutions tend to show higher transmittance due to less scattering and absorption of light.

At 421 nm, Ag-NPs exhibit SPR, causing them to transmit a significant amount of light. This leads to low transmittance at this wavelength. At other wavelengths, the nanoparticles do not absorb light as strongly, so more light passes through, leading to higher transmittance [28, 29].

2.8 | Antibacterial Activity of the AgNPs

AgNPs made from aqueous root extract of *Glycyrrhiza glabra* demonstrated excellent microbicidal activity when compared to

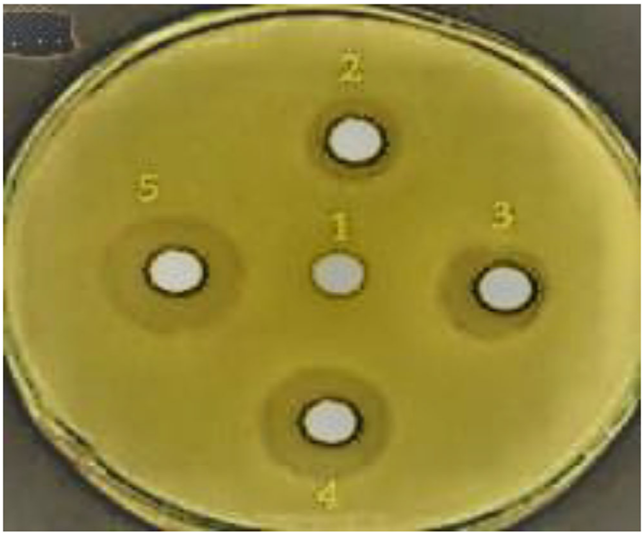

FIGURE 6 | Antibacterial activity of Ag-NPS synthesized from aqueous root extract of *Glycyrrhiza glabra* against *E. coli*.

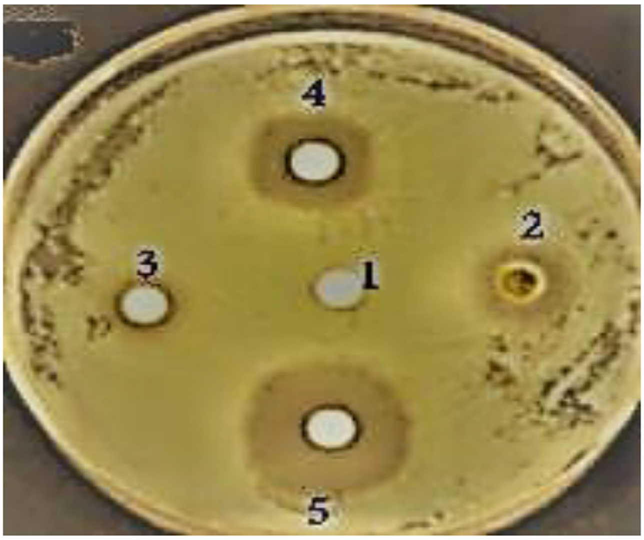

FIGURE 7 | Antibacterial activity of Ag-NPS synthesized from aqueous root extract of *Glycyrrhiza glabra* against *S. aureus*.

the standard negative control. A Gram-positive (*Staphylococcus aureus*) and a Gram-negative (*Escherichia coli*) strain were tested with produced AgNPs using the disc diffusion method as cited in Figure 6. The inhibitory zones were evaluated in terms of diameter to determine the antibacterial activity of aqueous root extracts of *Glycyrrhiza glabra* [30].

AgNPs have a microbicidal effect due to their tiny size and high surface-to-volume ratio. AgNPs have different antibacterial effects against Gram-negative (*E. coli*) and Gram-positive (*S. aureus*) bacteria, notwithstanding their competition for one over the other as shown in Figure 7. The antibacterial activity of Ag-NPs against Gram-negative and Gram-positive microbes has yielded inconsistent findings in earlier investigations [31–34]. The results show excellent antibacterial activity against both Gram-positive and Gram-negative bacteria. After measuring the zone of inhibition shows that the bio-synthesized Ag-NPs using

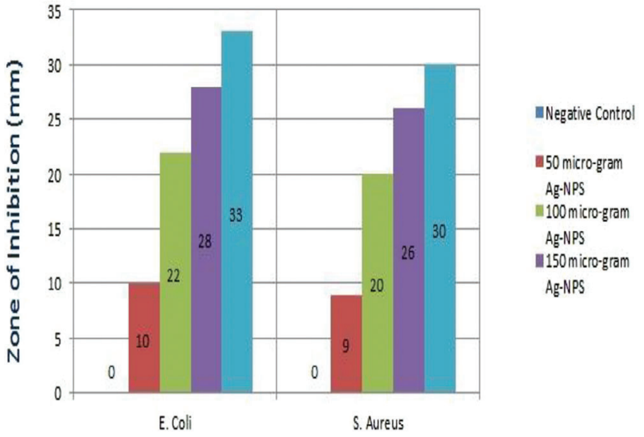

FIGURE 8 | Bar diagram showing microbicidal activity of AgNPs.

Glycyrrhiza glabra root extracts are more effective against Gram-negative (*E. coli*) bacteria than Gram-positive (*S. aureus*) bacteria. Ag-NPs are an inexpensive, environmentally benign, nontoxic, and efficient microbicidal agent that may also be utilized to treat human pathogenic bacteria and biofilms as shown in Figure 8.

The decreased transmittance in the visible region is a result of both the intrinsic optical characteristics of the Ag-NPs (like SPR) and their role in antimicrobial action, where light absorption aids in generating reactive species that harm microorganisms.

3 | Conclusion

In this study, Ag-NPs were successfully synthesized via sol–gel using the aqueous root extract of *Glycyrrhiza glabra*, demonstrating a green and sustainable approach to nanomaterial production. The XRD study confirmed the formation of Ag-NP with a standard card, and the XRD analysis indicated their crystalline structure and size. SEM study revealed the grain size of Ag-nanoparticle and found it to be an average of 81.24 nm. It is also observed at different scan rates that the grain size changes from 60 to 90 nm. SEM study also revealed the morphology of the prepared sample to be spherical shape and it is observed that Ag-NPs synthesized using plant extracts, the surface exhibited a slight roughness or a thin organic coating. The production of Ag-NPs is confirmed by energy dispersive x-ray analysis which reveals a strong signal in the silver region and noted that Ag and O made up 77.7 and 22.29 weight percent of the sample, respectively. The strong absorption of silver is noted in the range of visible region (421 nm) due to SPR and also confirmed the formation of monodispersed AgNPs. At 421 nm, Ag-NPs absorb a lot of light due to a phenomenon of SPR, which means less light gets through, resulting in low transmittance at this wavelength. However, at other wavelengths, the nanoparticles absorb less light, allowing light to pass through and leading to higher transmittance. AgNPs root extract of *Glycyrrhiza glabra* showed strong antibacterial activity compared to a control group. They were tested against two types of bacteria as follows: Gram-positive *Staphylococcus aureus* and Gram-negative *Escherichia coli*, using the disc diffusion method. The results showed that AgNPs effectively inhibited the growth of both types of bacteria, but they worked better against the Gram-negative *E. coli* due to the effectiveness of AgNPs comes from their small size and large surface area, which enhance their ability to kill bacteria. Overall, these Ag-NPs are a promising, safe, and eco-friendly option for combating harmful bacteria and could be useful in treating infections and preventing biofilms.

Acknowledgments

The authors extend their appreciation to King Saud University for funding this work through the Researchers Supporting Project number (RSP2025R378), King Saud University, Riyadh, Saudi Arabia.

Conflicts of Interest

The authors declare no conflicts of interest.

Data Availability Statement

The data that support the findings of this study are available from the corresponding author upon reasonable request.

References

1. Y. Ma, Y. Leng, D. Huo, et al., "A Portable Sensor for Glucose Detection in Huangshui Based on Blossom-Shaped Bimetallic Organic Framework Loaded With Silver Nanoparticles Combined With Machine Learning," *Food Chemistry* 429 (2023): 136850, https://doi.org/10.1016/j.foodchem.2023.136850.

2. L. Zhang, H. Shi, X. Tan, Z. Jiang, P. Wang, and J. Qin, "Ten-Gram-Scale Mechanochemical Synthesis of Ternary Lanthanum Coordination Polymers for Antibacterial and Antitumor Activities," *Frontiers in Chemistry* 10 (2022): 898324, https://doi.org/10.3389/fchem.2022.898324.

3. G. Zeng, Z. Wu, W. Cao, Y. Wang, X. Deng, and Y. Zhou, "Identification of Anti-Nociceptive Constituents From the Pollen of Typha Angustifolia L. Using Effect-Directed Fractionation," *Natural Product Research* 34, no. 7 (2020): 1041–1045, https://doi.org/10.1080/14786419.2018.1539979.

4. Y. Zhang, X. Zheng, Y. Liu, et al., "Effect of Oridonin on Cytochrome P450 Expression and Activities in HepaRG Cell," *Pharmacology* 101, no. 5-6 (2018): 246–254, https://doi.org/10.1159/000486600.

5. Y. Wang, S. Guo, W. Sun, et al., "Synthesis of 4H-Pyrazolo[3,4-d] Pyrimidin-4-One Hydrazine Derivatives as a Potential Inhibitor for the Self-Assembly of TMV Particles," *Journal of Agricultural and Food Chemistry* 72, no. 6 (2024): 2879–2887, https://doi.org/10.1021/acs.jafc.3c05334.

6. S. Chen, Z. Yang, W. Sun, K. Tian, P. Sun, and J. Wu, "TMV-CP Based Rational Design and Discovery of α-Amide Phosphate Derivatives as Anti Plant Viral Agents," *Bioorganic Chemistry* 147 (2024): 107415, https://doi.org/10.1016/j.bioorg.2024.107415.

7. H. Wu, J. Li, L. Tian, F. Zhao, J. Yin, and Y. Shao, "pH-Sensitive Phosphorescence in Penicillamine-Coated Au_{22} Nanoclusters: Theoretical and Experimental Insights," *Chemical Engineering Journal* 495 (2024): 153608, https://doi.org/10.1016/j.cej.2024.153608.

8. J. Wei, P. Fan, Y. Huang, et al., "(±)-Hypandrone A, a Pair of Polycyclic Polyprenylated Acylphloroglucinol Enantiomers With a Caged 7/6/5/6/6 Pentacyclic Skeleton From *Hypericum androsaemum*," *Organic Chemistry Frontiers*, 11, no. 12 (2024): 3459–3464. https://doi.org/10.1039/D4QO00444B.

9. L. Wang, H. Hu, and C.-C. Ko, "Osteoclast-Driven Polydopamine-to-Dopamine Release: An Upgrade Patch for Polydopamine-Functionalized Tissue Engineering Scaffolds," *Journal of Functional Biomaterials* 15, no. 8 (2024): 211, https://doi.org/10.3390/jfb15080211.

10. C. Feng, Y. Shi, J. Hao, et al., "Nuclear Magnetic Resonance Features of Low-Permeability Reservoirs With Complex Wettability," *Petroleum Exploration and Development* 44, no. 2 (2017): 274–279, https://doi.org/10.1016/S1876-3804(17)30030-7.

11. Y. Yao and S. Chen, "A Novel and Simple Approach to the Good Process Performance of Methane Recovery From Lignocellulosic Biomass Alone," *Biotechnology for Biofuels* 9 (2016): 115, https://doi.org/10.1186/s13068-016-0530-1.

12. X. Hou, L. Qiu, S. Luo, K. Kang, M. Zhu, and Y. Yao, "Chemical Constituents and Antimicrobial Activity of Wood Vinegars at Different Pyrolysis Temperature Ranges Obtained From *Eucommia Ulmoides* Olivers Branches," *RSC Advances* 8, no. 71 (2018): 40941–40949, https://doi.org/10.1039/C8RA07491G.

13. L. Qiu, Y. F. Deng, F. Wang, M. Davaritouchaee, and Y. Q. Yao, "A Review on Biochar-Mediated Anaerobic Digestion With Enhanced Methane Recovery," *Renewable and Sustainable Energy Reviews* 115 (2019): 109373, https://doi.org/10.1016/j.rser.2019.109373.

14. D. Wang, J. Ou-Yang, W. Guo, X. Yang, and B. Zhu, "Novel Fabrication of PZT Thick Films by an Oil-Bath Based Hydrothermal Method," *Ceramics International* 43, no. 12 (2017): 9573–9576, https://doi.org/10.1016/j.ceramint.2017.04.119.

15. L.-C. Zhao, Y. Liu, Z. Wang, et al., "Liquid Chromatography/Mass Spectrometry Analysis and Hepatoprotective Effect of Steamed Platycodi Radix on Acute Alcohol-induced Liver Injury," *International Journal of Pharmacology* 14 (2018): 952–962, https://doi.org/10.3923/ijp.2018.952.962.

16. C. Liu, Z. Li, H. Zhang, et al., "Visualization of the Elevated Levels of Hypochlorous Acid in Alzheimer's Disease With a Ruthenium(II) Complex-Based Luminescence Probe," *Analytica Chimica Acta* 1279 (2023): 341779, https://doi.org/10.1016/j.aca.2023.341779.

17. X. Ji, P. Jiang, Y. Jiang, et al., "Toward Enhanced Aerosol Particle Adsorption in Never-Bursting Bubble via Acoustic Levitation and Controlled Liquid Compensation," *Advancement of Science* 10 (2023): 2300049, https://doi.org/10.1002/advs.202300049.

18. H. Zhou, J. Guo, G. Zhu, H. Xu, X. Tang, and X. Luo, "Flotation Behavior and Mechanism of Smithsonite Under the System of Bidentate Ligand Sulfide Sodium Thiocyanate," *Separation and Purification Technology* 334 (2024): 126086, https://doi.org/10.1016/j.seppur.2023.126086.

19. M. Ijaz, M. Zafar, and T. J. I. Iqbal, "Green Synthesis of Silver Nanoparticles by Using Various Extracts: A Review," *Inorganic and Nano-Metal Chemistry* 51, no. 5 (2020), 744–755.

20. A. S. Jain, P. S. Pawar, A. Sarkar, V. Junnuthula, and S. Dyawanapelly, "Bionanofactories for Green Synthesis of Silver Nanoparticles: Toward Antimicrobial Applications," *International Journal of Molecular Sciences* 22, no. 21 (2021): 11993.

21. D. Jini and S. Sharmila, "Green Synthesis of Silver Nanoparticles From Allium Cepa and Its In Vitro Antidiabetic Activity," *Materials Today: Proceedings* 22 (2020): 432–438.

22. M. Junaid, Noor-ul-Ain, R. Jabeen, et al., "Iron-Doped Nickel Oxide as a Potential Biosensor of Urea Determination via Voltammetry," *Physica B: Condensed Matter* 651 (2023): 414592, https://doi.org/10.1016/j.physb.2022.414592.

23. M. Junaid, M. ul M. Shah, ul A. Noor, and M. Javed, "Hydrothermal Preparation of Iron Doped Nickel Oxide for Electrochemical Sensing of Urea," *Chemical Physics Impact* 3 (2021): 100052, https://doi.org/10.1016/j.chphi.2021.100052.

24. S. Khodadadi, N. Mahdinezhad, B. Fazeli-Nasab, M. J. Heidari, B. Fakheri, and A. Miri, "Investigating the Possibility of Green Synthesis of Silver Nanoparticles Using Vaccinium Arctostaphlyos Extract and Evaluating Its Antibacterial Properties," *BioMed Research International* 2021 (2021): 5572252.

25. M. Narayanan, S. Divya, D. Natarajan, et al., "Green Synthesis of Silver Nanoparticles From Aqueous Extract of Ctenolepis Garcini L. and Assess Their Possible Biological Applications," *Process Biochemistry* 107 (2021): 91–99.

26. M. K. Panda, N. K. Dhal, M. Kumar, P. M. Mishra, and R. K. Behera, "Green Synthesis of Silver Nanoparticles and Its Potential Effect on Phytopathogens," *Materials Today: Proceedings* 35 (2021): 233–238.

27. A. Q. Ahmad, N. Attique, R. Ali, et al., "Green Synthesis and Characterization of Fe/Mg Nanoparticles for Their Potential Applications Against Aflatoxogenic A. flavus," *Results in Chemistry* 7 (2024): 101312, https://doi.org/10.1016/j.rechem.2024.101312.

28. A. Salayová, Z. Bedlovičová, N. Daneu, et al., "Green Synthesis of Silver Nanoparticles With Antibacterial Activity Using Various Medicinal Plant Extracts: Morphology and Antibacterial Efficacy," *Nanomaterials (Basel)* 11, no. 4 (2021): 1005.

29. N. Swilam and K. A. Nematallah, "Polyphenols Profile of Pomegranate Leaves and Their Role in Green Synthesis of Silver Nanoparticles," *Scientific Reports* 10, no. 1 (2020): 1–11.

30. G. Tailor, B. Yadav, J. Chaudhary, M. Joshi, and C. Suvalka, "Green Synthesis of Silver Nanoparticles Using Ocimum Canum and Their Anti-Bacterial Activity," *Biochemistry and Biophysics Reports* 24 (2020): 100848.

31. M. Junaid, S. Ghulam Hussain, N. Abbas, and W. Q. Khan, "Band Gap Analysis of Zinc Oxide for Potential Bio Glucose Sensor," *Results in Chemistry*, 5, 2023, 100961, https://doi.org/10.1016/j.rechem.2023.100961.

32. C. Vanlalveni, S. Lallianrawna, A. Biswas, M. Selvaraj, B. Changmai, and S. L. Rokhum, "Green Synthesis of Silver Nanoparticles Using Plant Extracts and Their Antimicrobial Activities: A Review of Recent Literature," *Reviews in RSC Advances* 11, no. 5 (2021): 2804–2837.

33. H. Yousaf, A. Mehmood, K. S. Ahmad, and M. Raffi, "Green Synthesis of Silver Nanoparticles and Their Applications as an Alternative Antibacterial and Antioxidant Agents," *Materials Science and Engineering: C* 112 (2020): 110901.

34. M. Junaid, S. G. Hussain, N. U. Ain, R. Jabeen, W. Q. Khan, and N. Abbas, "Synthesis of Zinc Oxide Nanoparticles by Sol-Gel Method to Study Its Structural Optical Properties and Morphology," *Journal of Nanoscope* 3, no. 1 (2022): 29–36. 06/20.